Pulse-coupled distributed PLLs in heterogeneous wireless networks

O. Simeone(1) and G. Scutari(2)
(1)CWCSPR, New Jersey Institute of Technology,
University Heights, Newark, 07102-1982, USA
(2)Dept. INFOCOM, Univ. of Rome "La Sapienza",
via Eudossiana, 18, 00184 Rome, Italy

***Abstract*— Decentralized time synchronization in ad hoc or sensor networks can be conveniently achieved via pulse-coupled discrete-time phase locked loops (PLLs). Previous work has characterized (frequency or phase) synchronous states and convergence conditions for homogeneous networks where all the nodes have the same power constraints. In this paper, we build on recent results on algebraic graph theory for generally non-bidirectional graphs, and address the asymptotic behavior of pulse-coupled PLLs in heterogeneous networks. We first derive necessary and sufficient conditions for global synchronization of the network. Then, we provide closed form expressions for the asymptotic frequency and phases, as a function of the network topology.**

I. Introduction

Pulse-coupled distributed synchronization is a scalable and efficient solution to achieve coordination of local clocks in wireless networks that lack the presence of a central access point able to deliver timing information to *all* the participating nodes [1] [2]. With pulse coupling, local time information is communicated by each node to neighbors via the transmission of pulses aligned to the local clock. Different schemes have been advocated for the update of the local clock based on the pulses received from the neighbors: integrate-and-fire oscillators [1], linear filtering [2] and discrete-time Phase Locked Loops (PLLs) [3] [4] [5] (see also [6] where a similar model is studied for packet-coupled distributed synchronization [7]).

An important problem in distributed synchronization is that of predicting, given the topology of the network and the initial values of local frequencies and local phases of each clock, the steady-state of the system of coupled clocks and the related stability properties. Intuitively, steady-state and stability depend on the properties of the *connectivity graph* describing the inter-connections between different nodes. In the connectivity graph, a directed path exists between nodes i and j if the pulse transmitted from node j is received with sufficient power P_{ij} at node i (see, e.g., fig. 1). In particular, *strong connectivity*, i.e., the presence of a directed path (possibly composed of multiple edges) between any two nodes, appears to be a particularly favorable condition, since, with this, every node "sees" the local time of every other node, possibly through multiple hops[1]. Strong connectivity has been

[1]It is important to emphasize that strong connectivity does not require the presence of an edge between any two nodes, but only the presence of a path.

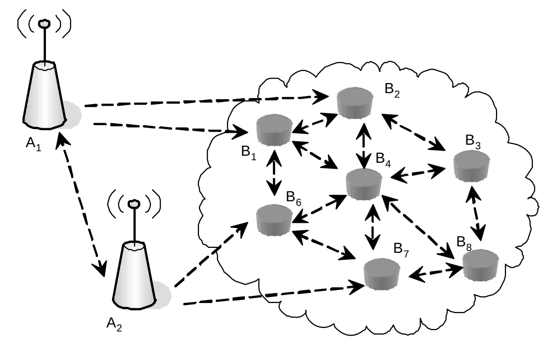

Fig. 1. A heterogeneous wireless network with nodes of class A and B.

shown to be a *sufficient* condition to achieve (asymptotically in the number of transmitted pulses): (*i*) *phase* synchronization in presence of frequency-synchronous local clocks for integrate-and-fire oscillators [8] and for discrete-time PLLs [5]; (*ii*) *frequency* synchronization (with generally mismatched phases) for the case of different local frequencies and discrete-time PLLs [5]. Moreover, it has been shown that, with a strongly connected graph, the steady-state value of the common phase (or frequency) is a convex combination of the initial phases (or frequencies) of all the nodes, where the combination coefficients depends on the graph topology [5]. It should be remarked that these results are analogous to the conditions derived for the convergence of distributed synchronization with analog PLLs [9], consensus problems in control (see, e.g., [10]) and distributed estimation [11].

While being a sufficient condition for synchronization, strong connectivity is known to be also *necessary* for the achievement of (frequency or phase) synchronization *only* in the case of *homogeneous* networks, where all the nodes transmit with the same power so that $P_{ij} = P_{ji}$ [5]. From an algebraic graph standpoint, this condition implies that the connectivity graph is *bidirectional:* the presence of an edge in one direction entails that an edge exists also in the other direction. However, many envisaged instances of ad hoc or sensor networks are heterogeneous in that nodes are often divided in different classes, say A and B, where class-A nodes have access to a larger power supply, so that in general $P_{ij} \neq P_{ji}$. An example of this scenario is a sensor network where access points (class-A nodes) are deployed in order to collect data from the active sensors (class-B nodes), see fig. 1. We emphasize that the sensor network is not all within the transmission range of the access points. In a heterogeneous networks, the connectivity graph is no longer bidirectional and strong connectivity is no longer a necessary condition for synchronization.

This paper focuses on pulse-coupled distributed synchronization based on discrete-time PLLs and attempts to fill the knowledge gap identified above by:

1) defining necessary and sufficient conditions for the achievement of (frequency or phase) synchronization in a heterogeneous wireless network;
2) characterizing the steady-state condition, i.e., the final value of the common frequency or phase, as a function of the topology of the given heterogenous wireless network.

Our analysis builds on recent results of [11] [12], which deal with distributed consensus over a directed graph. Our findings are finally validated via illustrative numerical results.

II. Pulse-coupled synchronization

In this section, we present the model of pulse-coupled synchronization via discrete-time PLLs in a heterogeneous network. For a more thorough presentation of the basic model of distributed discrete-time PLLs we refer the reader to [5]. We consider a network of N nodes, each endowed with a clock characterized by different free-oscillation frequencies $1/T_i$. Different nodes might belong to different classes and accordingly might have different available powers. This is accounted for by the power P_{ij} received by node i from node j, which can be written as

$$P_{ij} = \frac{C_{ij}}{d_{ij}^{\gamma}} G_j, \tag{1}$$

where $d_{ij} = d_{ji}$ is the distance between the nodes, γ is the path loss exponent ($\gamma = 2 \div 4$), $C_{ij} = C_{ji}$ is a channel-dependent coefficient that accounts for possible fading and shadowing and G_j accounts for the power transmitted by node j.

The ith clock is defined by a discrete-time function $t_i(n)$, that, in case of isolated (or uncoupled) nodes, evolves as $t_i(n) = nT_i + \theta_i(0)$, where index $n = 1, 2, ...$ runs over the periods of the clock and $0 \leq \theta_i(0) < T_i$ is an arbitrary initial phase. Notice that, in order to simplify the analysis, we are neglecting phase noise and frequency drifts [9]. Two synchronization conditions are of interest. We say the N clocks are *frequency* synchronized to a common frequency $1/T^*$ if $t_i(n+1) - t_i(n) = T^*$ for each i and for sufficiently large n. A stricter condition requires full *frequency and phase* synchronization, i.e., $t_1(n) = \cdots = t_N(n) = t^*(n)$ for n sufficiently large.

Towards the goal of achieving synchronization, clocks are coupled through the transmission by each node, say the jth, of a pulse at each tick of the local clock $t_j(n)$, either in a given dedicated bandwidth or spread spectrum code or in an overlay system such as UWB. Each node, say the ith, detects correctly only the pulses which are received with sufficient power, i.e., the pulse from node j is recorded at node i if $P_{ij} > \beta$ where β is a given threshold. Moreover, pulses are received after a propagation delays $q_{ij} = q_{ji}$. In this paper, for the sake of analysis, any node i is assumed to be able to evaluate the time of arrivals $t_{ij}(n) + q_{ij}$ for all the pulses j which are received with sufficient power $P_{ij} > \beta$. In [4] [5], practical solutions are proposed that remove this assumption.

Based on the time-difference measurements, the ith clock updates its instantaneous phase $\theta_i(n)$ in $t_i(n) = nT_i + \theta_i(n)$ according to a discrete-time PLL. In particular, a *timing error detector* estimates a convex combination of the "delayed" time differences $t_j(n) + q_{ij} - t_i(n)$ for $j \neq i$, at the nth period. Defining as $\alpha_{ij} \geq 0$ and $\sum_{j=1, j\neq k}^{K} \alpha_{ij} = 1$ the convex combination weights, we easily get that the output of the time error detector reads $\Delta t_i^{(Q)}(n+1) = \Delta t_i(n+1) + Q_i$, where the convex combination of (non-delayed) time differences is defined as

$$\Delta t_i(n+1) = \sum_{j=1, j\neq i}^{N} \alpha_{ij}(t_j(n) - t_i(n)) \tag{2}$$

and $Q_i = \sum_{j=1, j\neq i}^{N} \alpha_{ij} q_{ij}$. The measurement $\Delta t_i^{(Q)}(n+1)$ is fed to a loop filter $\varepsilon(z) = \varepsilon_0/(1 - \mu z^{-1})$, where $0 < \varepsilon_0 < 1$ denotes the loop gain and $0 \leq \mu < 1$ the loop pole. As it customary in the literature on PLLs (see, e.g., [14] [9]), we limit the scope to first ($\mu = 0$) and second ($\mu \neq 0$) - order PLLs. The output of filter $\varepsilon(z)$ drives the local Voltage Control Clock (VCC) as

$$\begin{aligned} t_i(n+1) - t_i(n) &= \varepsilon_0 \Delta t_i^{(Q)}(n+1) + \mu(t_i(n) - t_i(n-1)) \\ &\quad + (1-\mu)T_i \qquad \text{(3a)} \\ &= \varepsilon_0 \Delta t_i(n+1) + \mu(t_i(n) - t_i(n-1)) \\ &\quad + (1-\mu)T_i^{(Q)}. \qquad \text{(3b)} \end{aligned}$$

where $T_i^{(Q)} = T_i + \varepsilon_0 Q_i/(1-\mu)$.

A typical choice for the convex weights α_{ij} on which we will concentrate in the following is

$$\alpha_{ij} = \frac{P_{ij}}{\sum_{j=1, j\neq i}^{N} P_{ij}}, \tag{4}$$

as proposed in [3] and [4] for first-order discrete-time PLLs, with the convention that, if $\sum_{j=1, j\neq i}^{N} P_{ij} = 0$ (i.e., node i does not receive sufficient power from any other node j), we set $\alpha_{ij} = 0$ for all j.

III. System analysis

The system (3b) can be cast as the second-order vector difference equation

$$\mathbf{t}(n+1) = (\mathbf{A} + \mu \mathbf{I}) \cdot \mathbf{t}(n) - \mu \mathbf{t}(n-1) + (1-\mu)\mathbf{T}^{(Q)}, \tag{5}$$

where we defined the vectors $\mathbf{t}(n) = [t_1(n) \cdots t_N(n)]^T$ and $\mathbf{T} = [T_1^{(Q)} \cdots T_N^{(Q)}]^T$. Moreover, the system matrix reads

$\mathbf{A}=\mathbf{I}-\varepsilon_0\mathbf{L}$, with $\mathbf{L}$ being the graph Laplacian of the network: $[\mathbf{L}]_{ii}=\sum_{j\neq i}\alpha_{ij}=1$ (i.e., the in-degree of node i) and $[\mathbf{L}]_{ij}=-\alpha_{ij}$ for $i\neq j$. Notice that matrix $\mathbf{A}$ is stochastic: $\mathbf{A}\cdot\mathbf{1}=\mathbf{1}$ or equivalently $\mathbf{L}\cdot\mathbf{1}=\mathbf{0}$. Model (5) coincides with the framework considered in the literature on consensus of multi-agent networks for the special case $\mu=0$ and $\mathbf{T}^{(Q)}=\mathbf{0}$ [10]. In other words, the consensus model describes a scenario with first-order PLLs ($\mu=0$), no propagation delays and frequency synchronous clocks ($\mathbf{T}^{(Q)}=\mathbf{0}$).

A. Connectivity graph and some related definitions

The properties of distributed synchronization (described by (5)) in a given network depend critically on the connectivity among the participating nodes, which is captured by the connectivity graph $\mathcal{G}=\{\mathcal{N},\mathcal{E}\}$. The latter is a *directed graph* (or *digraph*) with set of vertices $\mathcal{N}=\{1,2,...,N\}$ given by the nodes of the networks and set of edges $\mathcal{E}=\{e_{ij}\colon \alpha_{ij}>0$ for $i,j=1,2,...,N\}$, each weighted by $\alpha_{ij}>0$ in (4). In other words, in our model, there exists a directed edge e_{ij} between two nodes i and j if and only if the power P_{ij} received by i from j is $P_{ij}>0$. Notice that the graph is *directed*, since we have in general $\alpha_{ij}\neq\alpha_{ji}$ for $i\neq j$, and *non-birectional*, that is $\alpha_{ij}=0$ does not imply $\alpha_{ji}=0$ for $i\neq j$. A few definitions are in order (for a more general presentation, the reader is referred to [12]). A *path*[2] between two nodes i and j is a sequence of nodes $\{i,n_1,n_2,...,n_{M,},j\}$ with $n_i\in\mathcal{N}$ such that (i,n_1), (n_i,n_{i+1}), $(n_M,j)\in\mathcal{E}$. A directed graph where there exists a path between any two nodes is said to be *strongly connected* (SC). A subgraph $\mathcal{G}_s=\{\mathcal{N}_s,\mathcal{E}_s\}\subseteq\mathcal{G}$ is said to be a *directed spanning tree* if it is a directed tree (i.e., there exists a *root node* that has a unique path towards all the other nodes in $\mathcal{N}_s$) and has the same node set as $\mathcal{G}$, $\mathcal{N}_s=\mathcal{N}$. In case $\mathcal{G}$ contains a directed spanning tree, we say that the directed graph is *quasi SC*. Finally, a directed graph $\mathcal{G}$ is said to be a *forest* if it consists of one or more directed trees.

In order to be able to define conveniently the properties of connectivity of a directed graph beside the basic ones listed above of strong connectivity and quasi strong connectivity, it is instrumental to introduce the concept of *condensation digraph* $\mathcal{G}^*=\{\mathcal{N}^*,\mathcal{E}^*\}$. The idea is that an arbitrary graph $\mathcal{G}$ can be partitioned into a number of subgraphs $\mathcal{G}_k=\{\mathcal{N}_k,\mathcal{E}_k\}\subseteq\mathcal{G}$ $(k=1,2,...,K)$, with $\mathcal{G}_i\cap\mathcal{G}_j=\oslash$ such that each $\mathcal{G}_k$ is SC. To see this, it is enough to notice that any node is SC so that each node in fact lies in a SC graph. Each subgraph $\mathcal{G}_k$ is referred to as a *SC component* (SCC) of the graph. Now, we build the condensation graph $\mathcal{G}^*$ by associating each SCC $\mathcal{G}_i$ with a single node in $\mathcal{N}^*$ and introducing a directed edge e^*_{ij} in $\mathcal{E}^*$ between of the ith and jth SCC ($\mathcal{G}_i$ and $\mathcal{G}_j$, respectively) if and only if there exists at least one edge from any node in $\mathcal{G}_i$ to any node in $\mathcal{G}_j$ in the original graph $\mathcal{G}$. If the condensation digraph $\mathcal{G}^*$ contains a spanning tree, we refer to the SCC at the root as the *root SCC* (RSCC). As we will see below, these definitions play a key role when studying the properties of convergence of distributed synchronization.

[2]In this paper, we do not consider weak paths [12] and thus refer to strong paths simply as paths for brevity.

B. Main results

We are first interested in finding general expression for (frequency or phase) synchronous steady states of system (5). To this end, let us denote a possible value for the synchronized frequency as $1/T^*$ and define the phases $\tau_i(n)$ relative to this frequency as $t_i(n)=nT^*+\tau_i(n)$. In vector form, the previous equation becomes $\mathbf{t}(n)=nT^*\cdot\mathbf{1}+\boldsymbol{\tau}(n)$ with $\boldsymbol{\tau}(n)=[\tau_1(n)\ \cdots\tau_N(n)]^T$. Frequency-synchronized states correspond to steady-state solutions $\mathbf{t}^*(n)$ of the form

$$\mathbf{t}^*(n)=nT^*\cdot\mathbf{1}+\boldsymbol{\tau}^*, \tag{6}$$

where full synchronization further requires the phase vector to satisfy $\boldsymbol{\tau}^*=\tau^*\mathbf{1}$, with τ^* being a common phase.

Lemma 1: Synchronous steady-state solutions (6) of the system (5) satisfy

$$T^*=\mathbf{v}^T\mathbf{T}, \tag{7}$$

with $\mathbf{v}$ being the normalized left eigenvector of matrix $\mathbf{A}$ corresponding to eigenvalue 1 ($\mathbf{A}^T\mathbf{v}=\mathbf{v}$ with $\mathbf{1}^T\mathbf{v}=1$) and

$$\mathbf{L}\boldsymbol{\tau}^*=(1-\mu)\frac{\boldsymbol{\Delta}\mathbf{T}^{(Q)}}{\varepsilon_0}, \tag{8}$$

with $[\boldsymbol{\Delta}\mathbf{T}^{(Q)}]_k=\mathbf{T}^{(Q)}-T^*\mathbf{1}$ being the frequency mismatch vector between initial local frequency (that accounts for delays) $T_k^{(Q)}$ and common frequency T^*.

Proof: Writing (5) as a function of the phases $\boldsymbol{\tau}(n)$, we easily obtain the vector difference equation

$$\boldsymbol{\tau}(n{+}1){-}\boldsymbol{\tau}(n){=}-\varepsilon_0\mathbf{L}\boldsymbol{\tau}(n){+}\mu(\boldsymbol{\tau}(n){-}\boldsymbol{\tau}(n{-}1))+(1{-}\mu)\boldsymbol{\Delta}\mathbf{T}^{(Q)}. \tag{9}$$

Imposing the condition $\boldsymbol{\tau}(n+1)=\boldsymbol{\tau}(n)=\boldsymbol{\tau}(n-1)=\boldsymbol{\tau}^*$ in (9), we immediately get (8), from which (7) follows by application of the equalities $\mathbf{v}^T{\cdot}\mathbf{L}=\mathbf{0}$ and $\mathbf{1}^T\mathbf{v}=1$. ■

From (8) (and the fact $\mathbf{L}\cdot\mathbf{1}=\mathbf{0}$), we see that phase synchronization (i.e., $\boldsymbol{\tau}^*=\tau^*\mathbf{1}$) is not achievable if a frequency mismatch or propagation delays are present, that is, if $\boldsymbol{\Delta}\mathbf{T}^{(Q)}\neq\mathbf{0}$.

1) First-order PLLs: In the following, we focus at first on first-order PLLs ($\mu=0$). We now review a necessary and sufficient condition for convergence in homogeneous networks.

Proposition 1: Consider first-order PLLs ($\mu=0$) and homogeneous networks (i.e., $P_{ij}=P_{ji}$). Convergence to a synchronous state of the form (6) (and thus (7)-(8)) is guaranteed if and only if the connectivity graph $\mathcal{G}$ is strongly connected. Moreover, the steady-state phase vector satisfies

$$\boldsymbol{\tau}^*=\mathbf{1}{\cdot}\eta{+}\frac{\mathbf{L}^\dagger}{\varepsilon_0}\boldsymbol{\Delta}\mathbf{T}^{(Q)}, \tag{10}$$

with $(\cdot)^\dagger$ denoting the pseudoinverse and

$$\eta{=}\,\mathbf{v}^T\left(\boldsymbol{\tau}(0)-\frac{\mathbf{L}^\dagger}{\varepsilon_0}\boldsymbol{\Delta}\mathbf{T}^{(Q)}\right). \tag{11}$$

Proof: Let us define $\boldsymbol{\tau}'(n)=\boldsymbol{\tau}(n)-\frac{\mathbf{L}^\dagger\boldsymbol{\Delta}\mathbf{T}}{\varepsilon_0}$. With this change of variables, the difference equation (9) boils down to

$$\boldsymbol{\tau}'(n+1)=\mathbf{A}\cdot\boldsymbol{\tau}'(n). \tag{12}$$

Convergence properties of system (12) (and in particular the steady-state solution (10)-(11)) can be directly obtained from Theorem 1 and 4 of [5]. In particular, to prove sufficiency, we use the well-known fact that strong connectivity implies that matrix $\mathbf{A}$ has a simple eigenvalue $\lambda_1 = 1$ (or equivalently the Laplacian matrix $\mathbf{L}$ has a simple zero eigenvalue), whereas all the other eigenvalues are such that $|\lambda_i| < 1$ so that $\boldsymbol{\tau}'(n) \to \mathbf{1}\mathbf{v}^T\boldsymbol{\tau}'(0)$ (see also [10]). ■

When considering Proposition 1, it should be remarked that strong connectivity is known to be only a sufficient condition for the achievement of synchronization in heterogeneous networks, for which the underlying connectivity graph is not bidirectional. We now consider a necessary and sufficient condition for convergence in heterogeneous networks.

Proposition 2. Consider first-order PLLs ($\mu = 0$) and a general (heterogenous) network. Convergence to a synchronous state of the form (6) (and thus (7)-(8)) is guaranteed if and only if the connectivity graph $\mathcal{G}$ contains at least a spanning directed tree (that is, if $\mathcal{G}$ is quasi SC). Moreover, under this assumption, the steady-state phase vector satisfies (10)-(11).

Proof: Given the change of variables used in the proof of Proposition 2, Proposition 3 follows directly from the results in [10] [13] [12], where it is shown that a necessary and sufficient condition for the Laplacian matrix to have a simple zero eigenvalue is the presence of spanning directed tree in the connectivity graph. ■

While the previous Propositions sheds light onto the role of graph topology on the convergence of the distributed synchronization algorithm, it does not clarify how the steady-state solution (7), (10)-(11) is affected by the network topology (connectivity). Notice that in order to characterize the steady-state behavior (7), (10)-(11), we should determine how the left eigenvector $\mathbf{v}$ corresponding to eigenvalue $\lambda_1 = 1$ of matrix $\mathbf{A}$ varies with the network topology.

Proposition 3. The ith component of vector $\mathbf{v}$ is strictly positive $v_i > 0$ if and only if node i is the root of a spanning directed tree for the connectivity graph $\mathcal{G}$.

Proof: Follows directly from the arguments used to prove Proposition 1 and 2 and the results in [12]. ■

The previous proposition brings evidence to a fairly intuitive phenomenon: only the nodes whose timing signal reaches (possibly through multiple hops) all the nodes in the network, that is the root nodes of spanning trees, contribute to the final value of the steady-state frequency (7) and phase (10)-(11).

Finally, we would like to comment on the possibility that the network fractionates in multiple clusters of frequency or phase synchronization. In other words, we are interested in finding conditions under which there exist subsets $\mathcal{G}_k$ of the original graph $\mathcal{G}$ composed of, say, $N_k < N$ nodes, such that, within $\mathcal{G}_k$, convergence of the system to steady-state solutions of the form (6) is guaranteed. One trivial conditions is that the subsets $\mathcal{G}_k$ consist of isolated components of the graph $\mathcal{G}$ (meaning that no edges exist to $\mathcal{G}_k$ from $\mathcal{G}\backslash\mathcal{G}_k$ and viceversa), which contain a spanning directed tree (recall Proposition 2). Excluding this trivial case, a necessary and sufficient condition for the appearance of clusters of synchronization is provided by the following Proposition.

Proposition 4. Consider first-order PLLs ($\mu = 0$) and a general (heterogenous) network with non-isolated components. Disjoint clusters of nodes $\mathcal{G}_k \subseteq \mathcal{G}$ ($k = 1, 2, ..., K$), with $\mathcal{G}_i \cap \mathcal{G}_j = \oslash$ for $i \neq j$, exist in which the timing vectors $\mathbf{t}_{\mathcal{G}_k}(n) = [t_i(n)]_{i\in\mathcal{G}_k}$ converge to synchronous solutions of the form $\mathbf{t}^*_{\mathcal{G}_k}(n) = nT^*_{\mathcal{G}_k} \cdot \mathbf{1} + \boldsymbol{\tau}^*_{\mathcal{G}_k}$ with

$$T^*_{\mathcal{G}_k} = \mathbf{v}^T_{\mathcal{G}_k}\mathbf{T}^{(Q)}_{\mathcal{G}_k} \tag{13}$$

and

$$\boldsymbol{\tau}^* = \mathbf{1}\cdot\mathbf{v}^T_{\mathcal{G}_k}\left(\boldsymbol{\tau}_{\mathcal{G}_k}(0) - \frac{\mathbf{L}^\dagger_{\mathcal{G}_k}}{\varepsilon_0}\boldsymbol{\Delta}\mathbf{T}^{(Q)}_{\mathcal{G}_k}\right) + \frac{\mathbf{L}^\dagger_{\mathcal{G}_k}}{\varepsilon_0}\boldsymbol{\Delta}\mathbf{T}^{(Q)}_{\mathcal{G}_k}, \tag{14}$$

(the subscript $\mathcal{G}_k$ identifies restriction of the corresponding quantity to subgraph $\mathcal{G}_k$) if and only if the following conditions are satisfied: (*i*) each $\mathcal{G}_k$ is a RSCC for the condensation graph of $\mathcal{G}$; (*ii*) the condensation graph of $\mathcal{G}$ is a forest.

Proof: Follows directly from [12] and Proposition 3. ■

2) Second-order PLLs: While second order PLLs have the potential to reduce of the steady-state phase error (as it is clear from (8)), convergence of the system (5) is not always guaranteed if the pole μ is sufficiently large. This is in accordance with well known results for conventional point-to-point PLLs. While at the moment we do not have conditions for convergence as in the first-order case discussed above, we can provide a characterization of the steady-state synchronous solutions (6).

Proposition 5. Consider second-order PLLs ($\mu > 0$) and a general (heterogenous) network. A synchronous solution of the form (6) (and thus (7)-(8)) satisfies

$$\boldsymbol{\tau}^* = \mathbf{1}\cdot\mathbf{v}^T\left(\boldsymbol{\tau}(0) - (1-\mu)\frac{\mathbf{L}^\dagger}{\varepsilon_0}\boldsymbol{\Delta}\mathbf{T}^{(Q)}\right) + (1-\mu)\frac{\mathbf{L}^\dagger}{\varepsilon_0}\boldsymbol{\Delta}\mathbf{T}^{(Q)}. \tag{15}$$

Proof: Similarly to Proposition 1, consider the change of variables $\boldsymbol{\tau}'(n) = \boldsymbol{\tau}(n) - (1-\mu)\frac{\mathbf{L}^\dagger\boldsymbol{\Delta}\mathbf{T}}{\varepsilon_0}$ in (9). The resulting system is a second-order vector difference equation, that can be studied by recasting it as a first-order vector difference equation in terms of vector $\tilde{\boldsymbol{\tau}}(n) = [\boldsymbol{\tau}'(n)^T \;\; \boldsymbol{\tau}'(n-1)^T]^T$ with system matrix

$$\tilde{\mathbf{A}} = \begin{bmatrix} \mathbf{A}+\mu\mathbf{I} & -\mu\mathbf{I} \\ \mathbf{I} & \mathbf{0} \end{bmatrix}. \tag{16}$$

Convergence of the corresponding system

$$\tilde{\boldsymbol{\tau}}(n) = \tilde{\mathbf{A}}\tilde{\boldsymbol{\tau}}(n-1)$$

depends on the eigenvalues of $\tilde{\mathbf{A}}$. It is easy to see that $\tilde{\mathbf{A}}$ has an eigenvalue equal to one, with left and (normalized) right eigenvectors $\mathbf{z}_\ell = \mathbf{1}$ and $\mathbf{z}_r = 1/(1-\mu)[\mathbf{v}^T \; -\mu\mathbf{v}^T]^T$. Therefore, the system (12) is stable if and only if all the remaining $2K-1$ eigenvalues of $\tilde{\mathbf{A}}$ have absolute value less than one (see, e.g., [10]). Assuming that the stability condition mentioned above holds (which is not always the case, as discussed above), then we have $\tilde{\mathbf{A}}^n \to \mathbf{z}_\ell\mathbf{z}_r^T$ for $n \to \infty$ (see, e.g., [10]) and the phases $\boldsymbol{\tau}'(n)$ converge as

$\boldsymbol{\tau}'(n) \to \mathbf{1}\mathbf{v}^T\boldsymbol{\tau}'(0)$, from which (15) follows (see also [5]). ■

From (15), the potential reduction in the static phase error due to the presence of the pole is apparent. It is also important to remark that the results of Propositions 3 and 4 on the contribution of different nodes to the synchronous state (15) for different network topologies apply verbatim to the case of second-order PLLs. This is due to the fact that the results of Propositions 3 and 4 only depend on the properties of the left eigenvector $\mathbf{v}$ of the Laplacian matrix $\mathbf{L}$. In the next section, our conclusions are corroborated via numerical results.

IV. Numerical results

We consider the distributed wireless networks sketched in the upper parts of figures 2-5, where we have $N_B = 16$ nodes of class B (gray dots) regularly placed on square of size 1 and a different number N_A of nodes of class A (black dots) ($N = N_A + N_B$). The received power (1) is characterized by $C_{ij} = 1$, path loss exponent $\gamma = 3$ and the transmit power is $G_j = 1$ for nodes of class B and $G_j = 8$ for nodes of class A. Moreover, the power threshold for pulse detection is set to $\beta = (N_B/2)^{\gamma/2}$ in order to allow correct reception of a pulse sent by a class-B node by the eight class-B nodes surrounding it. These choices create the connectivity graphs shown in the upper parts of figures 2-5. Parameters of the second-order PLLs are selected as $\varepsilon_0 = 0.9$, $\mu = 0.3$. Finally, initialization of the local oscillators is carried out by considering frequency synchronous clocks, $T_1 = ... = T_N = 1$, and initial phases equi-spaced in the interval $(0, 1)$.

Figures 2-5 consider four scenarios characterized by different number N_A of class-A nodes, respectively $N_A = 0, 1, 2, 4$, and plot the phases $\boldsymbol{\tau}(n)$ of the different (class-A and class-B) nodes versus time n. Class-A node phases are shown in dashed lines and class-B node phases in solid lines. These experiments are mainly meant to corroborate the results in Propositions 3 and 4 about the impact of topology on synchronization. We start with fig. 2, where the connectivity graph is SC and, accordingly, the phases $\boldsymbol{\tau}(n)$ synchronize to a common value that depend on all the initial phases $\boldsymbol{\tau}(0)$: moreover, since the graph is balanced (that is, $1 = \sum_{j \neq i} \alpha_{ij} = \sum_{j \neq i} \alpha_{ji}$), it can be easily shown that the common phase is simply the arithmetic average of all the initial phases [5] . In the scenario of fig. 3, the connectivity graph contains only one spanning directed tree, with root in the class-A node: as expected from Proposition 3, the phases of all nodes synchronize to the initial phase of the class-A node. Fig. 4 considers a network with two class-A nodes, where the connectivity graph contains a forest with two spanning trees, each having one class-A nodes as root. Accordingly (and by symmetry), convergence occurs to the arithmetic average of the initial phases of the two class-A nodes. Finally, fig. 5 corresponds to a scenario where the condensation graph of the connectivity graph contains a forest with two directed trees, having each as RSCC the two class-A nodes on either side. Therefore, as per Proposition 4, the phases within the RSCCs synchronize, which implies pairwise synchronization between the nearby class-A nodes,

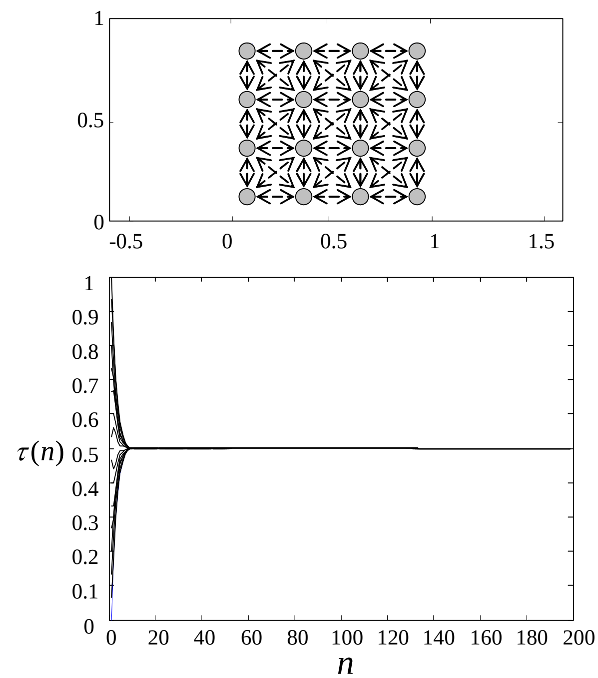

Fig. 2. Connectivity graphs (upper figure) and convergence of the local phases versus time (lower figure) with $N_A = 0$ class-A nodes (frequency-synchronous clocks, $\varepsilon_0 = 0.9$ and $\mu = 0.3$).

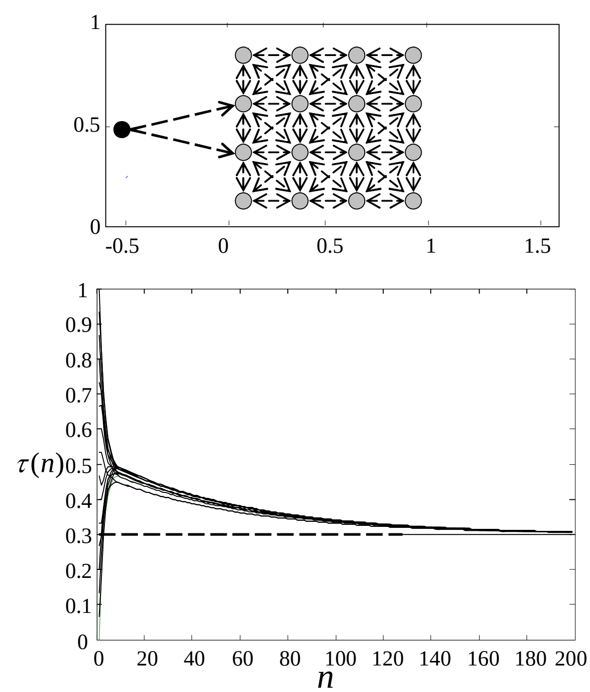

Fig. 3. Connectivity graphs (upper figure) and convergence of the local phases versus time (lower figure) with $N_A = 1$ class-A nodes (frequency-synchronous clocks, $\varepsilon_0 = 0.9$ and $\mu = 0.3$).

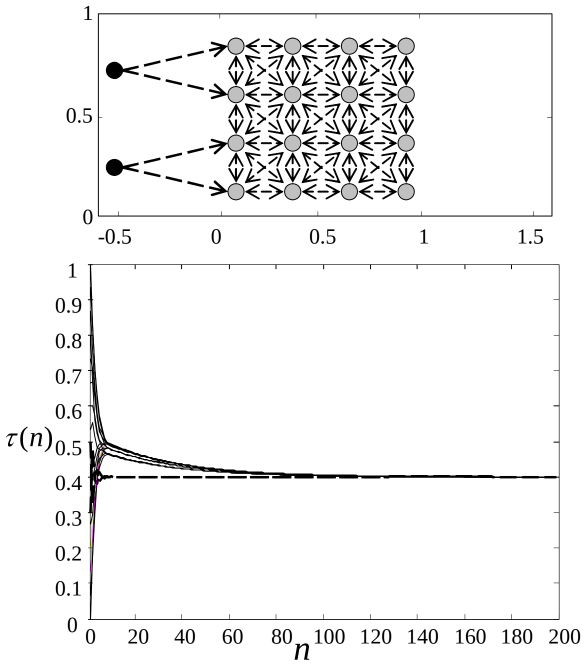

Fig. 4. Connectivity graphs (upper figure) and convergence of the local phases versus time (lower figure) with $N_A = 2$ class-A nodes (frequency-synchronous clocks, $\varepsilon_0 = 0.9$ and $\mu = 0.3$).

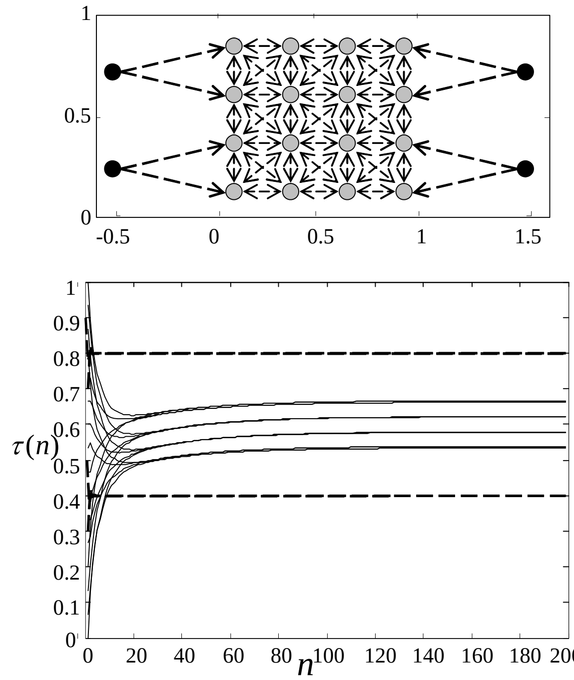

Fig. 5. Connectivity graphs (upper figure) and convergence of the local phases versus time (lower figure) with $N_A = 4$ class-A nodes (frequency-synchronous clocks, $\varepsilon_0 = 0.9$ and $\mu = 0.3$).

but in general synchronization does not occur for the other nodes.

V. Conclusions

In this paper, time synchronization via pulse-coupled PLLs has been studied for heterogeneous distributed wireless networks, where participating nodes can have different power constraints. The analysis derives necessary and sufficient conditions for frequency or phase synchronization of distributed first-order PLLs, and presents a characterization of steady-state synchronous solutions for both first and second-order PLLs. The results illuminate the impact of network topology on the performance of time synchronization, thus providing useful guidelines for the deployment of infrastructure-enhanced distributed networks (e.g., sensors networks with access points or fusion centers).

References

[1] Y.-W. Hong, A. Scaglione, "A scalable synchronization protocol for large scale sensor networks and its applications," *IEEE Journal Selected Areas Commun.*, vol. 23, no. 5, pp. 1085-1099, May 2005.

[2] An-Swol Hu and S. D. Servetto, "On the scalability of cooperative time synchronization in pulse-connected networks," *IEEE Trans. Inform. Theory*, vol. 52, no. 6, pp. 2725-2748, June 2006.

[3] F. Tong and Y. Akaiwa, "Theoretical analysis of interbase-station synchronization systems," *IEEE Trans. Commun.*, vol. 46, no. 5, pp. 590-594, 1998.

[4] E. Sourour and M. Nakagawa, "Mutual decentralized synchronization for intervehicle communications." *IEEE Trans. Veh. Technol.*, vol. 48, no. 6, pp. 2015-2027, Nov. 1999.

[5] O. Simeone and U. Spagnolini, "Distributed time synchronization in wireless sensor networks with coupled discrete-time oscillators," *Eurasip Journ. on Wireless Commun. and Networking*, vol. 2007, Article ID 57054, 13 pages, 2007.

[6] Qun Li and D. Rus, "Global clock synchronization in sensor networks," *IEEE Trans. Computers*, vol. 55, no. 2, pp. 214-226, Feb. 2006.

[7] F. Sivrikaya and B. F. Yener, "Time synchronization in sensor networks: a survey," *IEEE Network*, vol. 18, no. 4, pp. 45-50, July-Aug. 2004.

[8] D. Lucarelli and I-J. Wang, "Decentralized synchronization protocols with nearest neighbor communication," *in Proc. ACM SenSys 2004*, Baltimore, Nov. 2004.

[9] W. C. Lindsey, F. Ghazvinian, W. C. Hagmann and K. Desseouky, "Network synchronization," *Proc. of the IEEE*, vol. 73, no. 10, pp. 1445-1467, Oct. 1985.

[10] Wei Ren, R. W. Beard and E. M. Atkins, "A survey of consensus problems in multi-agent coordination," in *Proc. American Control Conference*, vol. 3, pp. 1859-1864, June 2005.

[11] S. Barbarossa, G. Scutari, "Bio-inspired sensor network design: Distributed decision through self-synchronization", *IEEE Signal Processing Magazine*, Volume 24, Issue 3, pp 26-35, May 2007.

[12] G. Scutari, S. Barbarossa and L. Pescosolido, "Distributed decision through self-synchronizing sensor networks in presence of propagation delays and nonreciprocal channels," in *Proc. SPAWC 2007.*

[13] Chai Whah Wu, "On Rayleigh-Ritz ratios of a generalized Laplacian matrix of directed graphs," *Linear Algebra and its applications*, vol. 402, pp. 207-227, 2005.

[14] F. M. Gardner, *Phaselock Techniques*, John Wiley & Sons, Inc., 1966.

[15] R. E. Mirollo and S. H. Strogatz, "Synchronization of pulse-coupled biological oscillators" *SIAM Journal on Applied Mathematics*, vol. 50, no. 6, pp. 1645-1662, Dec. 1990.

[16] L. Moreau, "Stability of multiagent systems with time-dependent communication links," *IEEE Trans. Automatic Control*, vol. 5, no. 2, pp. 169-181, Feb. 2005.

[17] R. D. Brualdi and H. J. Ryser, *Combinatorial matrix theory*, Cambridge University Press, 1991.